

## IUESIPS Processing on the VAX 8350

*Joy Nichols-Bohlin*

*June 20, 1988*

Since the time of launch of the IUE, standard processing of the data has been performed on a dedicated Xerox Sigma-9 computer. On February 16, 1988, the standard processing system for IUE data (IUESIPS) moved permanently to the VAX 8350 at GSFC. The conversion of IUESIPS to a VAX computer was initiated in anticipation of the final reprocessing of the entire IUE archive, which could not have been completed in a reasonable amount of time using the Sigma-9 computer, and to provide a final IUESIPS software package which runs on a widely used computer. In addition, the Sigma-9 computer is becoming increasingly unreliable and difficult to maintain with age. The Sigma-9 will continue to be used as the operations backup computer and for development of new operations software, such as the one-gyro mode.

The VAX IUESIPS software is a rehosting of the Sigma-9 code to Fortran 77. The code has been implemented in MIDAS (Munich Image Data Analysis System), and thus uses standard I/O interfaces and standard IDD (Image Display Device) interfaces. MIDAS provides a user-friendly environment for the operation of IUESIPS and the standard testing of software. The algorithms from the Sigma-9 code have been totally preserved; therefore, any differences between data processed on the VAX and data processed on the Sigma-9 should reflect inherent differences in the computational architecture of the two machines.

Compatibility testing was performed to compare the output data from the Sigma-9 and VAX IUESIPS, prior to implementation of the new VAX IUESIPS on February 16. Thirty-four images were chosen to be processed on both computers to test each of the processing schemes for the two default cameras. These images were carefully selected to represent a wide range of anomalies that can occur in the data, with the intent of fully exercising the software. The raw and photometrically corrected (PI) data were compared pixel-by-pixel and the differences were noted. The fluxes, epsilons, and wavelengths of the line-by-line data were compared. Also, the fluxes, epsilons, and wavelengths for each of the extracted files for both low and high dispersion were compared. Differences in "record 0" and the header label were identified and corrected.

The Sigma-9 computer truncates during real calculations, while the VAX rounds during these calculations. This basic difference in the machine architectures causes small differences in the final output data values computed during identically coded algorithms. The magnitude of the differences can be predicted from the number of calculations performed by a given algorithm. The initial worst case prediction for differences between the final output data values of the Sigma-9 IUESIPS and the VAX IUESIPS was  $\pm 9$  FN for the flux values of the PI, ELBL, MELO and MEHI files. This prediction took into account only the differences expected from truncation vs. rounding. Sources of additional differences discovered during

testing include the following:

1. Mathematical functions may be implemented differently on the two computers. For example, the square root of two is different at the seventh decimal place, a much larger difference than would be predicted based on the difference in precision of the two machines.
2. The nature of pixel data. Small differences in the calculations, when used to define a spatial position on the image for any reason (starting position for extraction, next extraction point in low dispersion, dispersion constants) can result in the selection or at least increased weighting of the neighboring pixel for the purpose of determining flux assignments or wavelength assignments. Since pixel-to-pixel variations cannot, as a rule, be predicted, isolated variations outside the initially predicted tolerances can occur.

Specifically, differences beyond the expected tolerances (all of which can be explained by differences in the computational architecture of the two computers) were found to be the following:

#### LOW DISPERSION DIFFERENCES:

1. Differences of  $\pm 2$  FN in the PI image, except for a single pixel at the edge of the photo-metrically corrected swath which is corrected on one computer and uncorrected on the other.
2. Differences of  $\pm 9$  FN in the ELBL and MELO fluxes, with occasional differences up to  $\pm 30$  FN in regions of extreme flux gradient on a very few images.
3. Slight apparent shift in wavelength between the net spectra from the two systems. This difference is due to slightly (0.01 pixel) different starting positions for the extraction process, based on differences in the calculated dispersion constants.
4. In the LWP camera,  $2464.0\text{\AA}$  on the Sigma-9 data is always assigned  $2464.2\text{\AA}$  on the VAX data. This is due to an inherent precision difference which manifests itself rarely (in fact, never in the SWP camera data).

#### HIGH DISPERSION DIFFERENCES:

1. Differences of  $\pm 2$  FN in the PI image
2. Differences in the high-dispersion net spectra increasing from zero at the beginning of each order to 5 FN at the end of each order. This difference results in an increasing difference in the ripple-corrected fluxes from zero at the beginning of each order to 30-80 FN at the end of each order. For data which have been extracted as extended source rather than point source (i.e., using a larger slit height), the differences are greater: 30 FN at the ends of the orders in the net fluxes and 100 FN or more at the ends of the order in the ripple-corrected fluxes. The source of these differences is the calculation of the smoothed background which is subtracted from the gross flux to produce the net flux. The effect of the truncation in the Sigma-9 calculation of the 31-point mean filtered data is increasing differences for each point from the beginning to the end of the order.

This was the only case where it was impossible to reproduce the calculating activity of the Sigma-9 in the conversion of IUESIPS to the VAX.

3. Occasional spikes of 5000 or more FN in the gross, background and net differences (NOT necessarily in the spectra themselves), again due to sampling a neighboring pixel based on slight differences in precision.
4. Wavelength assignments different by as much as  $0.012\text{\AA}$ .

Examples of the differences found during the compatibility testing are shown graphically in Figures 1-16. Two of the test images, LWP 12242 obtained at low dispersion and SWP 20166 obtained at high dispersion, have been chosen to demonstrate the nature of the differences. Figures 1-8 refer to LWP 12242 and Figures 9-16 refer to SWP 20166. Figures 1,3,5, and 7 show the difference in FN value at each point in the low dispersion extracted spectrum for the gross, background, net and absolutely calibrated net, respectively. Figures 2,4,6 and 8 are the corresponding histograms for these difference plots. Note that most of the data points differ by less than 9 FN, which was the initial predicted maximum difference between data processed on these two computer systems.

To show the differences encountered in the high dispersion spectra, two orders in the image SWP 20166 have been selected, 86 and 88. Figures 9-12 are plots of the differences in FN for each point in order 86, with the corresponding histogram, for the gross, background, net, and ripple-corrected net, respectively. Figures 13-16 show the same data for order 88. In order 86, the maximum difference in FN in the gross spectrum between data processed on the two computers is  $\pm 4.4$  FN (Figure 9). A spike in the difference occurs at  $1605\text{\AA}$  in the background difference spectrum for this order (Figure 10). The cause of this spike is documented in #3 above for high dispersion spectra. When the background is smoothed prior to subtraction from the gross spectrum to obtain the net spectrum, the spike is also smoothed, becoming shallower and broader. The net spectrum for order 86 shows this effect (Figure 11). Also barely visible in the net spectrum difference plot is a slight decline in the FN difference near the end of the order. The magnitude of the decrease, which indicates the FN values from the Sigma-9 processing are increasing with respect to the values from the VAX processing, is about 5 FN at the end of the order. The cause of this decrease is documented in #2 above, for high dispersion spectra. After application of the sinc function in the ripple correction, the difference is magnified, becoming as large as 80 FN at the end of the order in the ripple-corrected difference spectrum (Figure 12). Figure 13 shows a spike in the difference with a value of 1954 FN at  $1567\text{\AA}$  in order 88. This spike is seen in the net and ripple-corrected net as well (Figures 15 and 16). This is another example of a spike in the difference spectrum, but this time in the gross instead of the background differences. Orders 86 and 88 have been included to show the varying effects of spikes originating in the gross and in the background difference spectra.

The scientific staff at the IUE Observatory has concluded that the differences present between data processed on the Sigma-9 and the VAX will have no impact on the scientific data, and that data processed on the two computers are fully comparable. The differences are generally  $\leq 0.03\%$  of the flux. Occasionally, an individual point may differ by 0.5%, for

very low flux values. As always, extreme care is urged in the analysis of very weak spectral features ( $\leq 10\text{m}\text{\AA}$ ) or continuum fluxes that are weak and/or noisy. For comparison, the repeatability of IUE data is about  $\pm 3\%$ .

The VAX IUESIPS has been implemented only at GSFC. VILSPA continues to use the Sigma-9 version of IUESIPS. The two stations will continue to remain compatible in the sense that changes to one system will be converted to also run on the software at the other station. This situation should be especially noted by Principal Investigators of collaborative programs and GOs using archival data from both stations.

GO tapes created on the VAX 8350 are so indicated on their physical label. The origin of the data can also be easily determined by examining the header label of the data. Attached are copies of the labels from data processed on the Sigma-9 computer (Figure 17) and data processed on the VAX computer (Figure 18). Note that the final line of the header (with the suffix HL) reads ARCHIVE for data processed on the Sigma-9 and GOT\_FMTOUTTAPE for data processed on the VAX. These names reflect the names of the applications programs used by the two systems to write the output tapes. Also, you will probably notice that the names of all the applications programs have changed.

IUE Guest Observers may now request their processed data on FITS format tape as well as the original GO format tape. The FITS format currently supplied by the IUE Project at GSFC is a generic FITS produced in the MIDAS environment. No image or table extensions are used, and each extracted high dispersion order is a separate FITS file. The complete header information is not available on this generic FITS format; thus, both a FITS tape and the traditional GO tape will be provided to the Guest Observers who request FITS at this time. In the future, an IUEFITS format will be available with all of the header information preserved. This format, which has already been defined and approved by the Three Agencies, contains image and table extensions. When implemented, it will be provided instead of the traditional GO formatted tape upon request. Please note that at the time of the move of IUESIPS to the VAX, 1600bpi density became the default for GO magnetic tapes. The observer has the option, however, of requesting 800bpi or 6250bpi magnetic tapes instead of 1600bpi.

In summary, the IUESIPS production processing activities at GSFC were permanently moved to the VAX 8350 on February 16, 1988. Extensive compatibility testing between data processed on the Sigma-9 computer and data processed on the VAX computer was performed prior to the implementation of the VAX IUESIPS. Small differences in the processed data exist, due to the fact that the Sigma-9 computer is a truncating machine and the VAX is a rounding machine, as well as to other inherent computational differences, and to the effect of these differences on positional calculations for pixel data. These differences in the data should have no impact on the scientific compatibility or utility of the data from the two computers. The VAX IUESIPS has been implemented only at GSFC; VILSPA continues to use the Sigma-9 version of IUESIPS.

I will be happy to answer any question you may have concerning the processing of your IUE data. My phone number is (301) 286-5765 and my e-mail address is IUE::NICHOLS (SPAN). Please let me know if I can be of assistance.

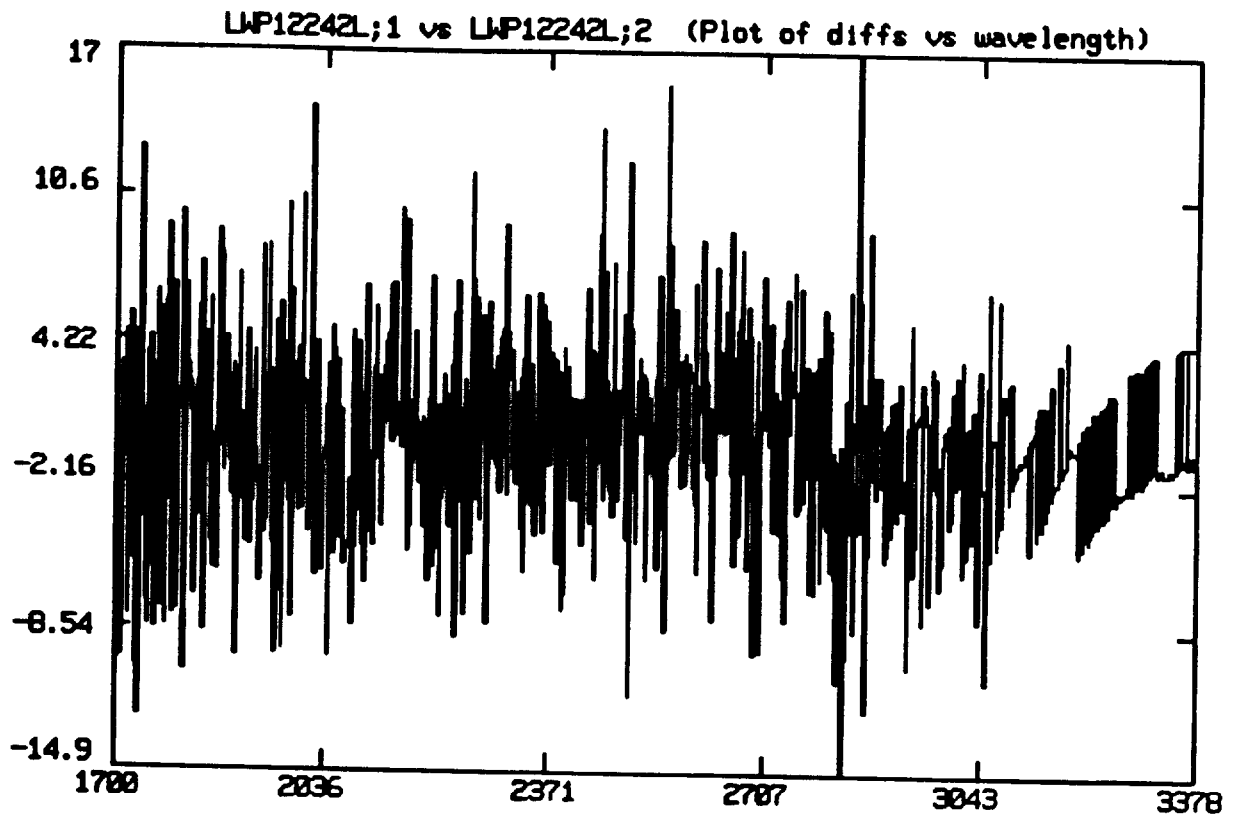


Figure 1: Plot of the difference in FN in the gross low dispersion spectrum of LWP 12242 between data processed on the VAX and data processed on the Sigma-9. The y-axis is in units of FN and the x-axis in units of Angstroms.

GROSS FLUX ORDER NO. 1 BIN WIDTH 1.0  
Minimum Difference = -14.922  
Maximum Difference = 16.977  
2 out of 901 values were identical

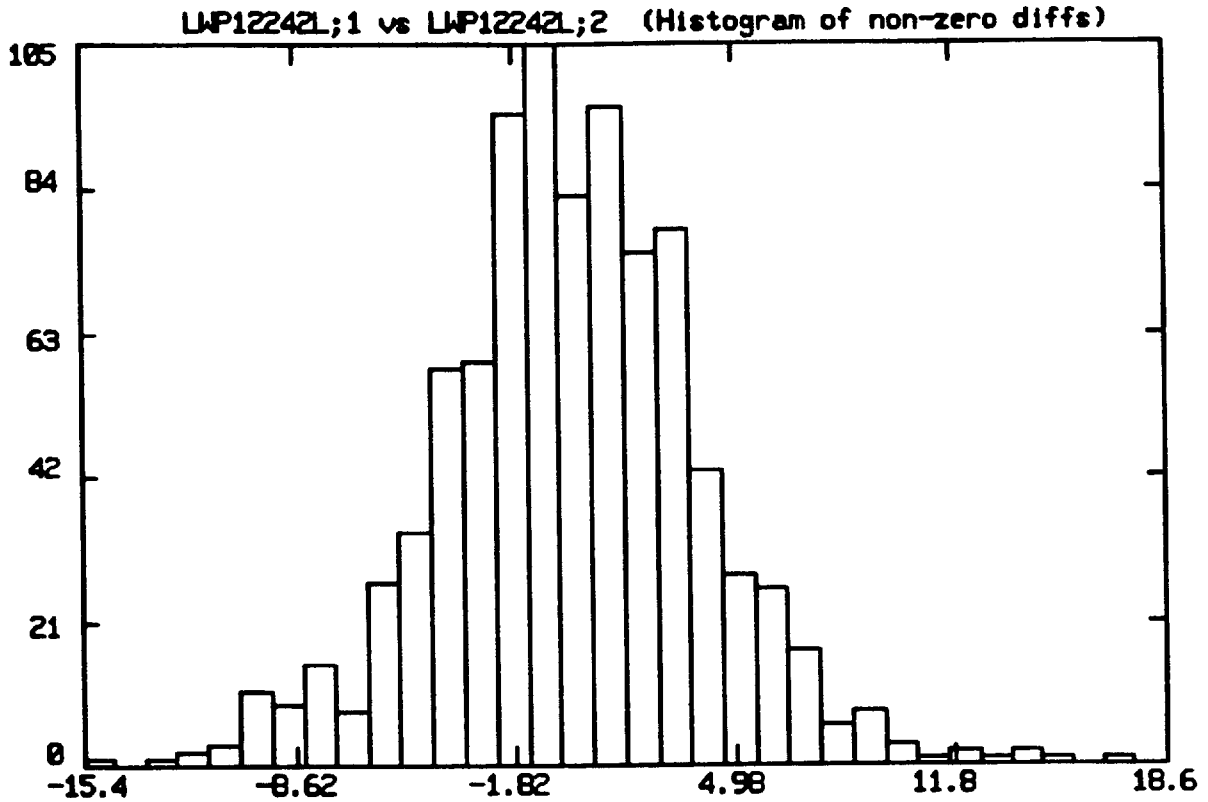


Figure 2: Histogram of the difference in FN in the gross low dispersion spectrum of LWP 12242 between data processed on the VAX and data processed on the Sigma-9. The y-axis is number of points and the x-axis is in units of FN difference.

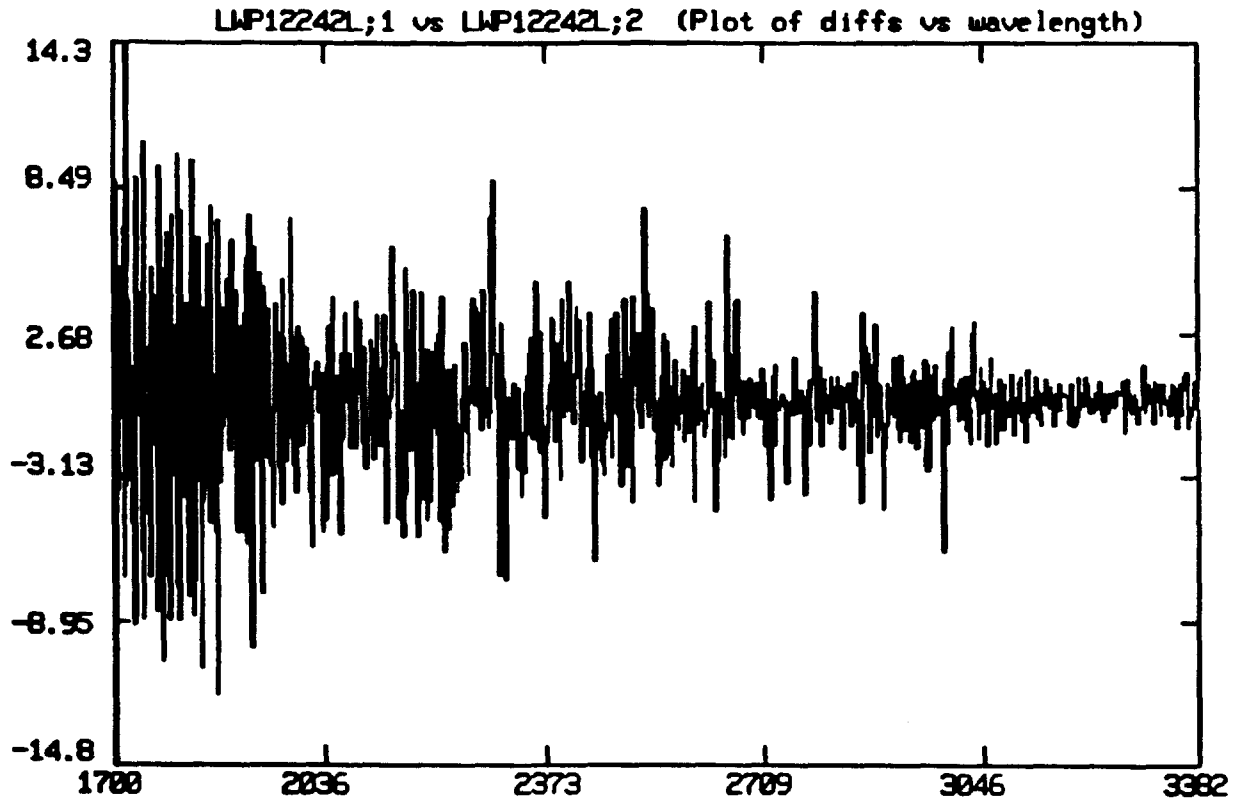


Figure 3: Plot of the difference in FN in the background low dispersion spectrum of LWP 12242 between data processed on the VAX and data processed on the Sigma-9. The y-axis is in units of FN and the x-axis in units of Angstroms.

BACKGROUND FLUX ORDER NO. 1 BIN WIDTH 1.0  
 Minimum Difference = -14.756  
 Maximum Difference = 14.297  
 1 out of 901 values were identical

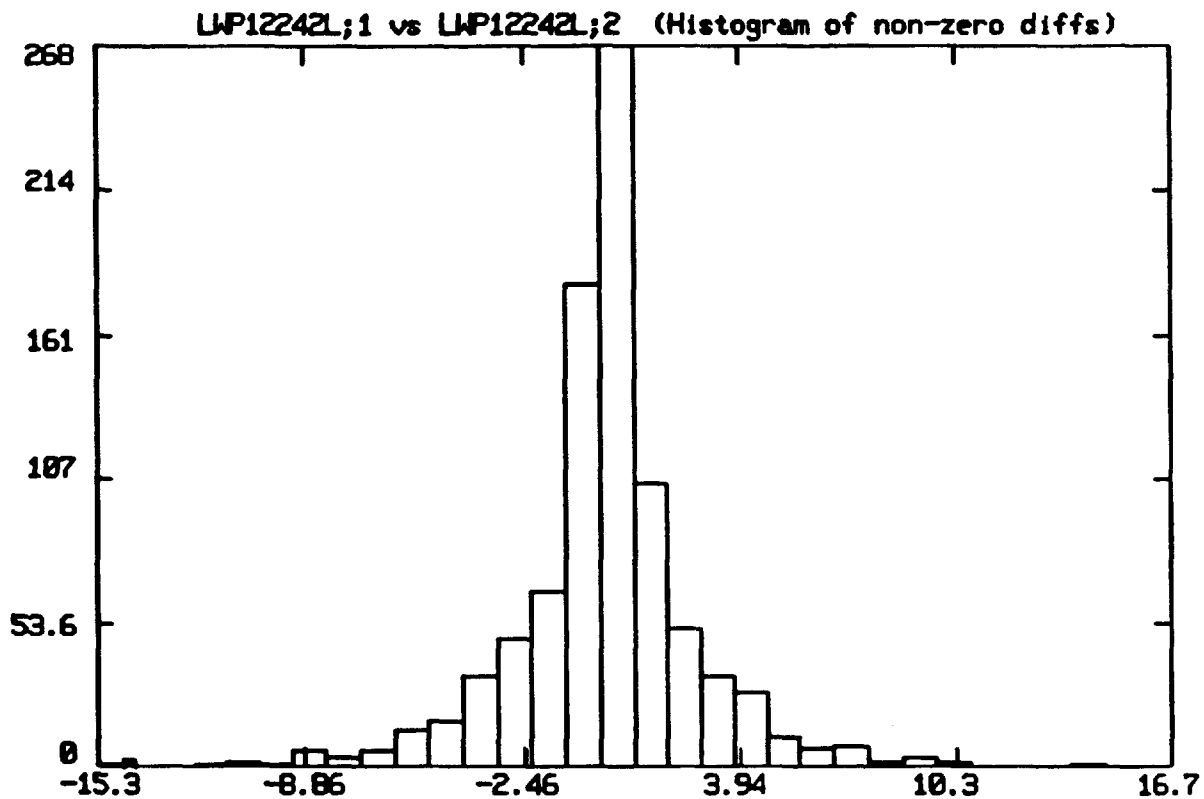


Figure 4: Histogram of the difference in FN in the background low dispersion spectrum of LWP 12242 between data processed on the VAX and data processed on the Sigma-9. The y-axis is number of points and the x-axis is in units of FN difference.



NET FLUX ORDER NO. 1

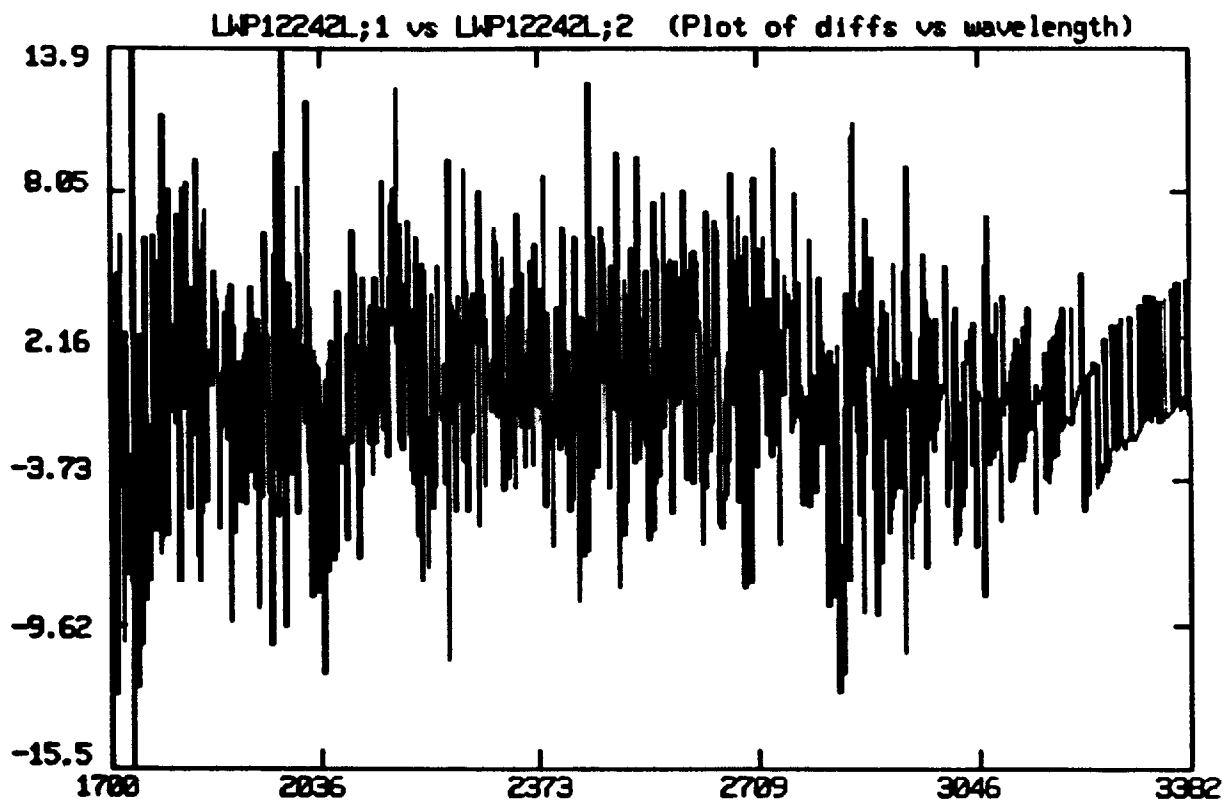


Figure 5: Plot of the difference in FN in the net low dispersion spectrum of LWP 12242 between data processed on the VAX and data processed on the Sigma-9. The y-axis is in units of FN and the x-axis in units of Angstroms.

NET FLUX ORDER NO. 1 BIN WIDTH 1.0  
Minimum Difference = -15.584  
Maximum Difference = 13.937  
1 out of 901 values were identical

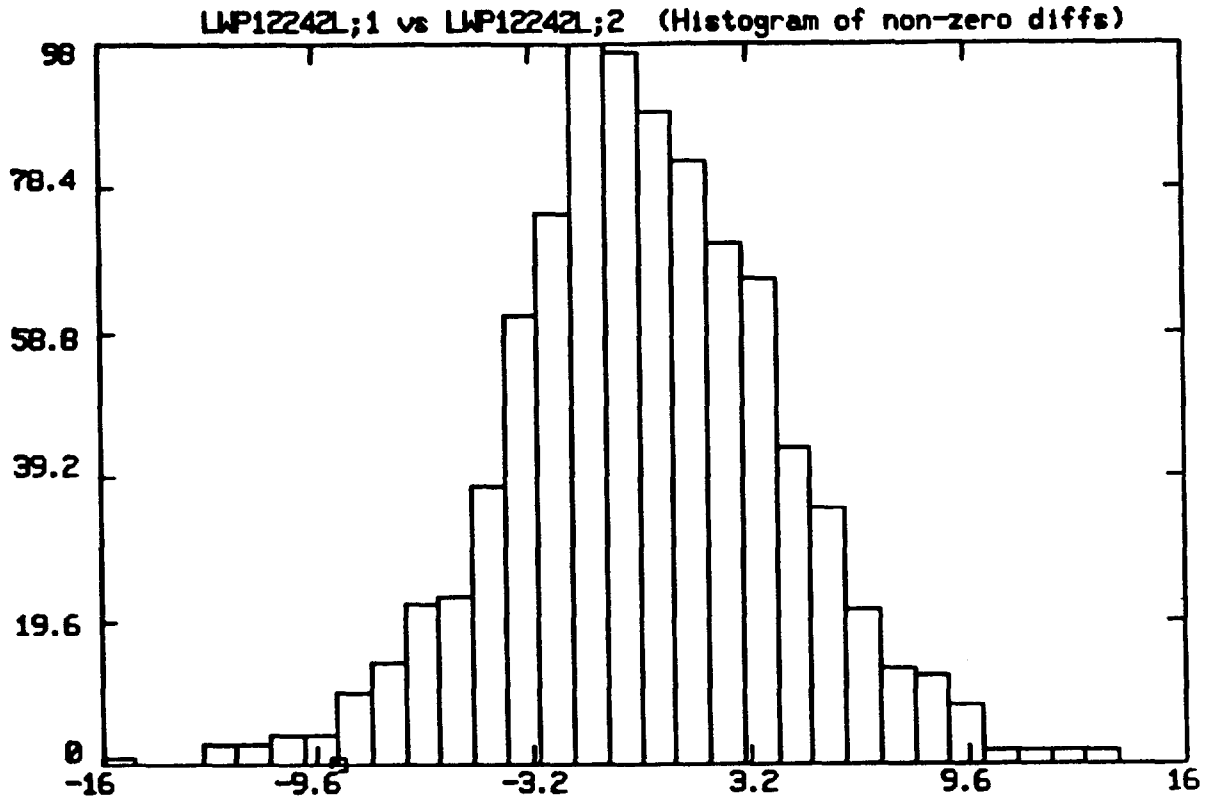


Figure 6: Histogram of the difference in FN in the net low dispersion spectrum of LWP 12242 between data processed on the VAX and data processed on the Sigma-9. The y-axis is number of points and the x-axis is in units of FN difference.

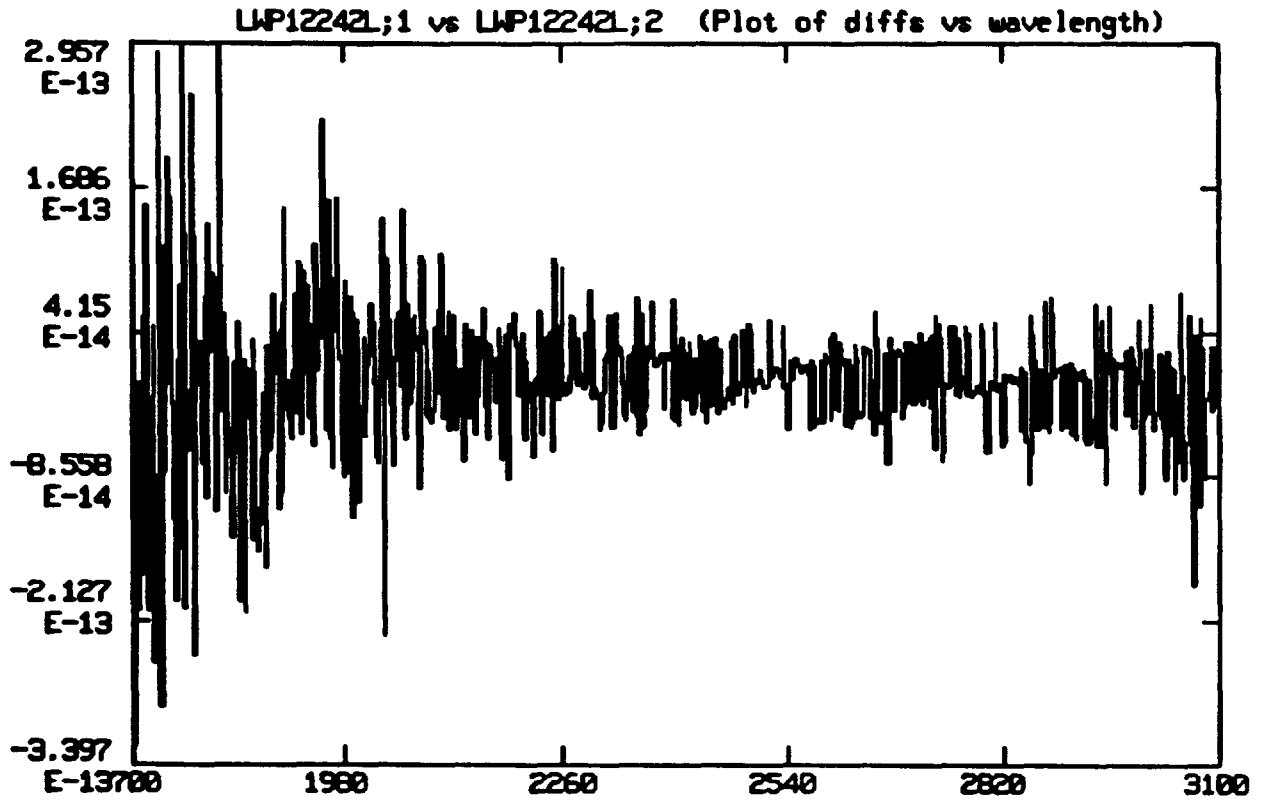


Figure 7: Plot of the difference in flux in the absolutely calibrated low dispersion spectrum of LWP 12242 between data processed on the VAX and data processed on the Sigma-9. The y-axis is in absolute flux units of ergs per square centimeter per second per Angstrom, and the x-axis in units of Angstroms.

ABS CALIB FLUX    ORDER NO. 1    BIN WIDTH 0.0  
 Minimum Difference = -3.39728E-13  
 Maximum Difference = 2.95652E-13  
 151 out of 901 values were identical

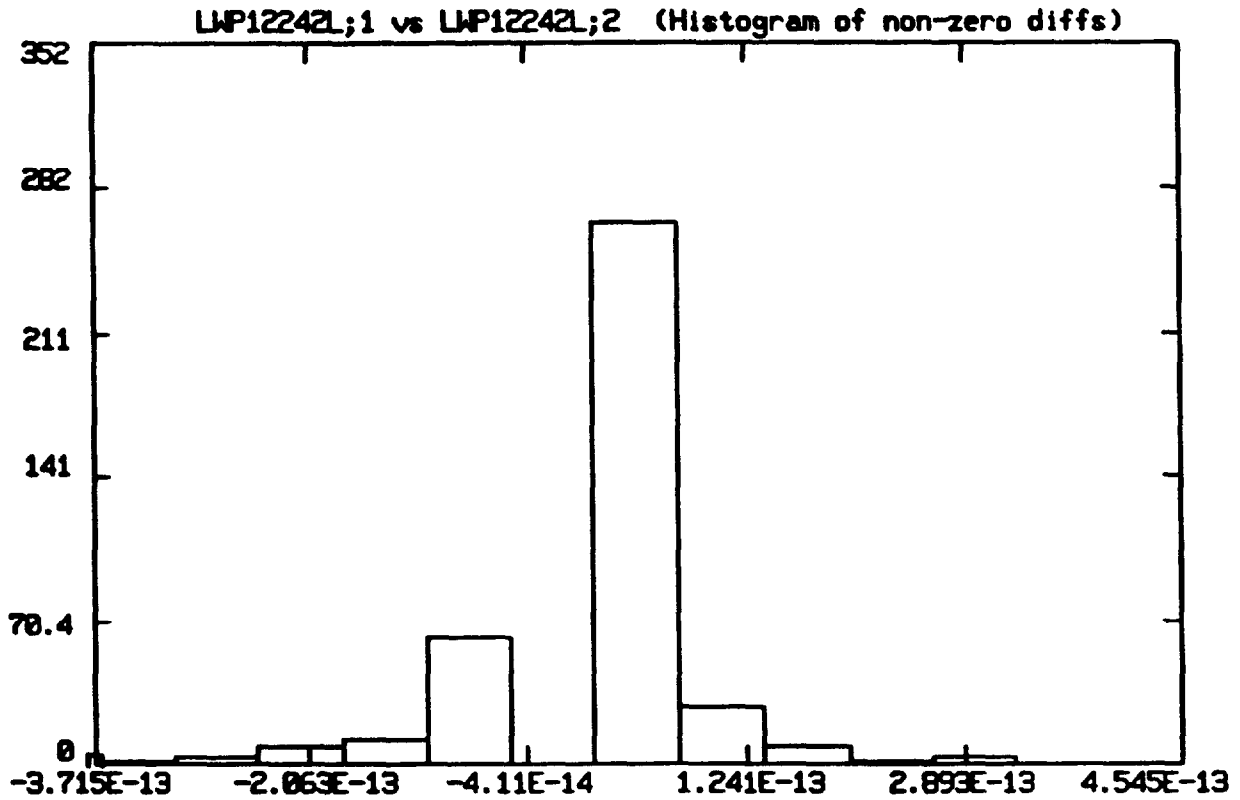


Figure 8: Histogram of the difference in flux in the absolutely calibrated low dispersion spectrum of LWP 12242 between data processed on the VAX and data processed on the Sigma-9. The y-axis is number of points and the x-axis is in units of absolute flux difference in ergs per square centimeter per second per Angstrom.

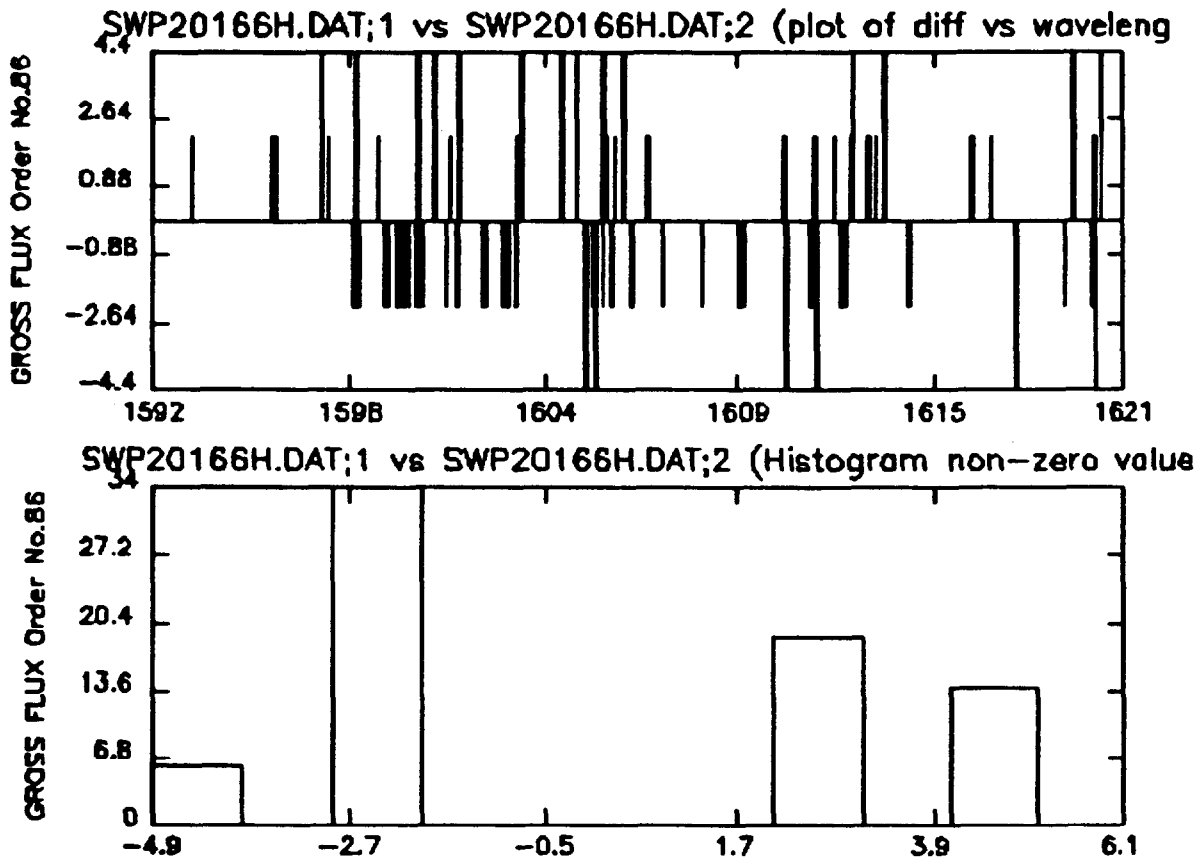


Figure 9: The top plot is the difference in FN in the gross high dispersion spectrum of SWP 20166, order 86, between data processed on the VAX and data processed on the Sigma-9. The y-axis is in units of FN and the x-axis in units of Angstroms. The bottom plot is the histogram of the difference in FN in the gross high dispersion spectrum of SWP 20166, order 86, between data processed on the VAX and data processed on the Sigma-9. The y-axis is number of points and the x-axis is in units of FN difference.

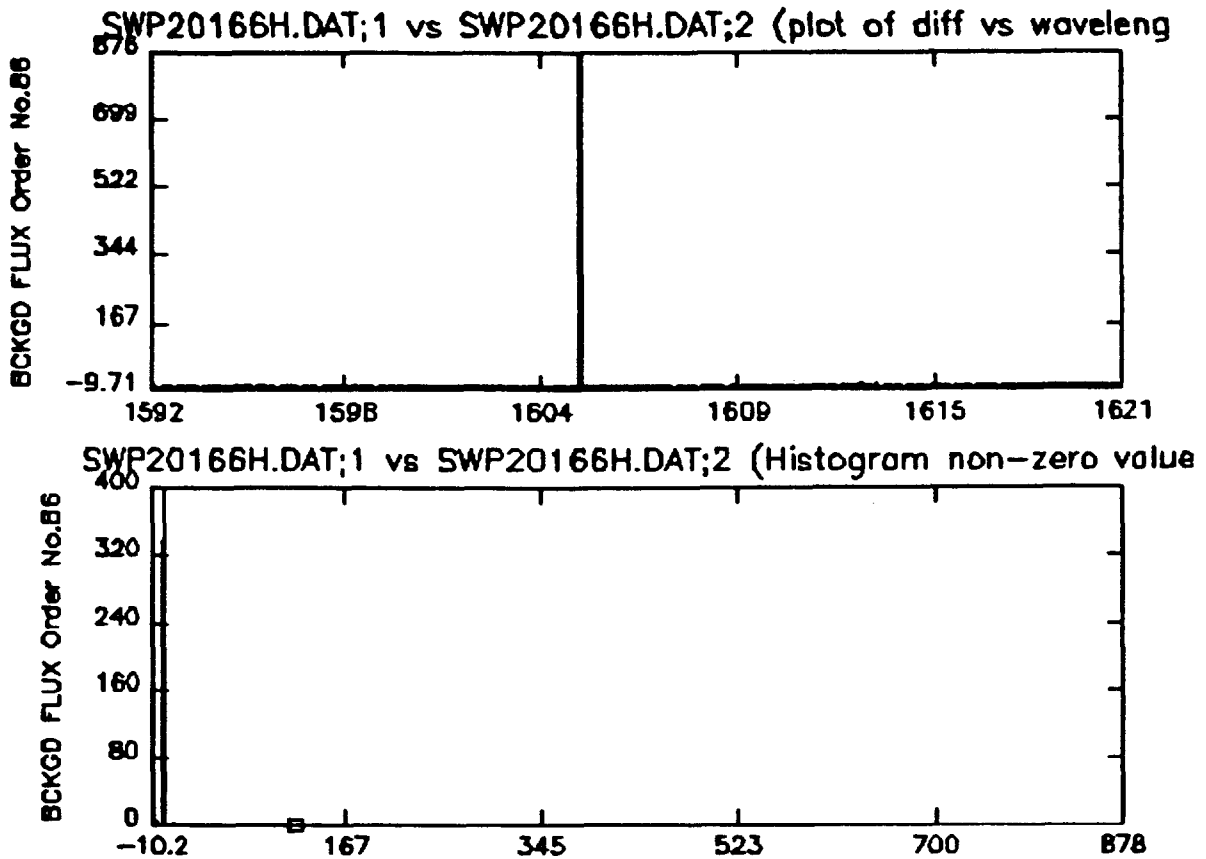


Figure 10: The top plot is the **difference** in FN in the background high dispersion spectrum of SWP 20166, order 86, between data processed on the VAX and data processed on the Sigma-9. The y-axis is in units of FN and the x-axis in units of Angstroms. The bottom plot is the histogram of the **difference** in FN in the background high dispersion spectrum of SWP 20166, order 86, between data processed on the VAX and data processed on the Sigma-9. The y-axis is number of points and the x-axis is in units of FN difference. Note the spike in the difference at 1605Å caused by differences in precision between the two computers.

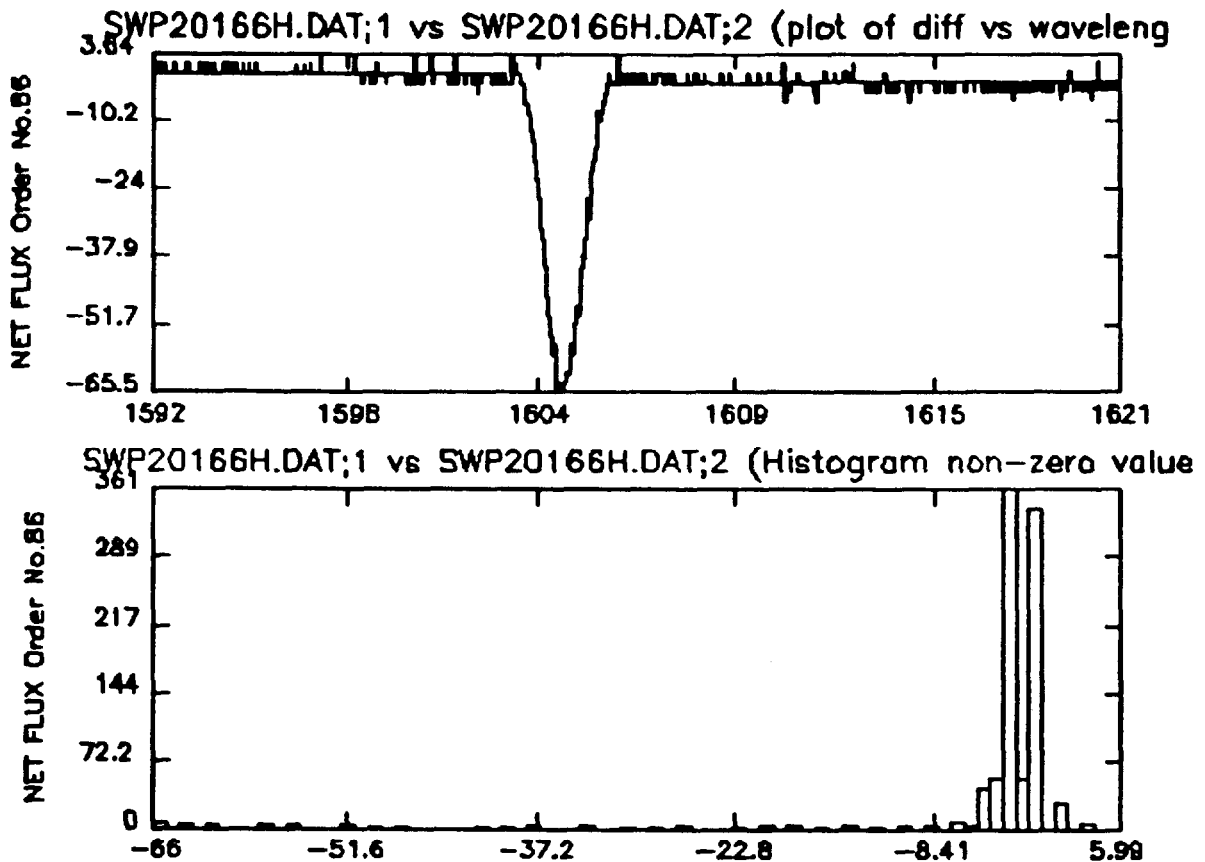


Figure 11: The top plot is the difference in FN in the net high dispersion spectrum of SWP 20166, order 86, between data processed on the VAX and data processed on the Sigma-9. The y-axis is in units of FN and the x-axis in units of Angstroms. The bottom plot is the histogram of the difference in FN in the net high dispersion spectrum of SWP 20166, order 86, between data processed on the VAX and data processed on the Sigma-9. The y-axis is number of points and the x-axis is in units of FN difference. The spike has become broader and shallower because the background is smoothed and then subtracted from the gross spectrum to obtain the net spectrum.

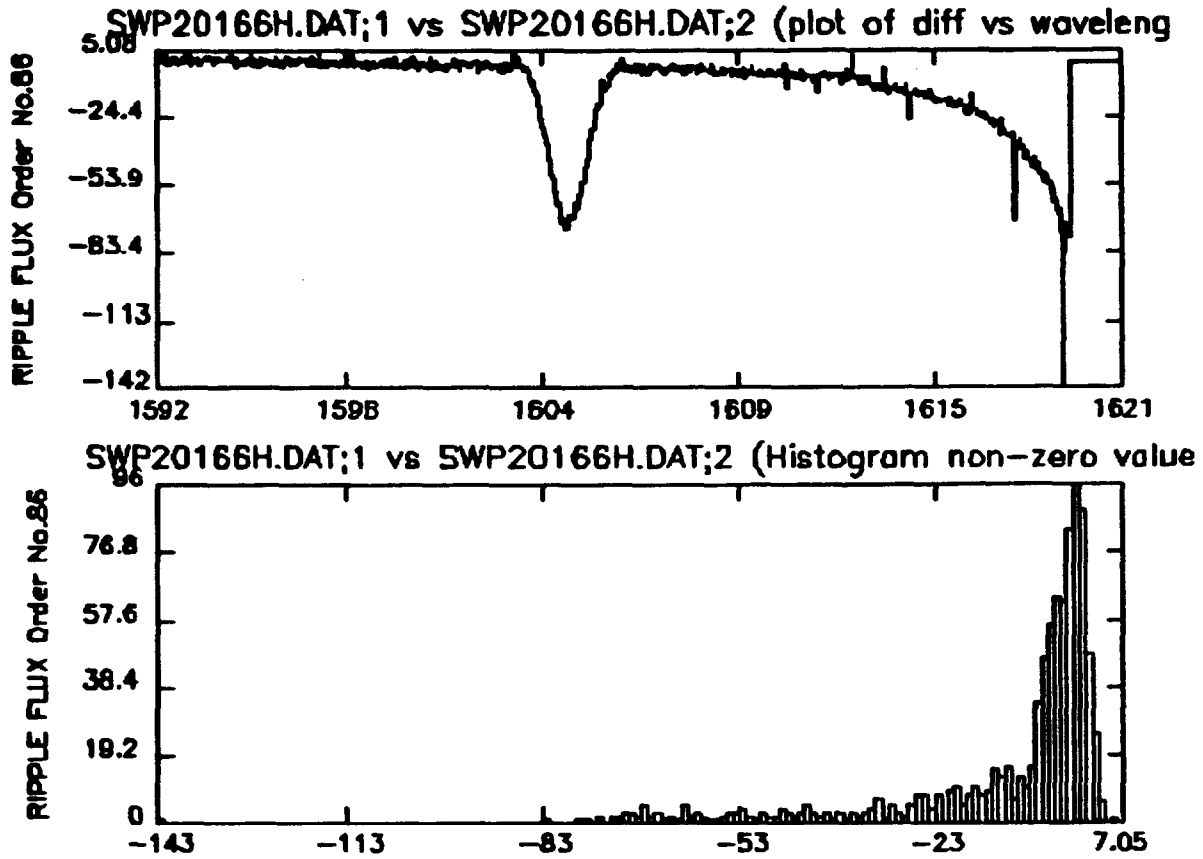


Figure 12: The top plot is the difference in FN in the ripple-corrected high dispersion spectrum of SWP 20166, order 86, between data processed on the VAX and data processed on the Sigma-9. The y-axis is in units of FN and the x-axis in units of Angstroms. The bottom plot is the histogram of the difference in FN in the ripple-corrected high dispersion spectrum of SWP 20166, order 86, between data processed on the VAX and data processed on the Sigma-9. The y-axis is number of points and the x-axis in units of FN difference. The effect of the spike in the background is still apparent. In addition, the difference in the FN becomes more negative (the FN values from the Sigma-9 are greater than the FN values from the VAX) towards the end of the order. See text for explanation.



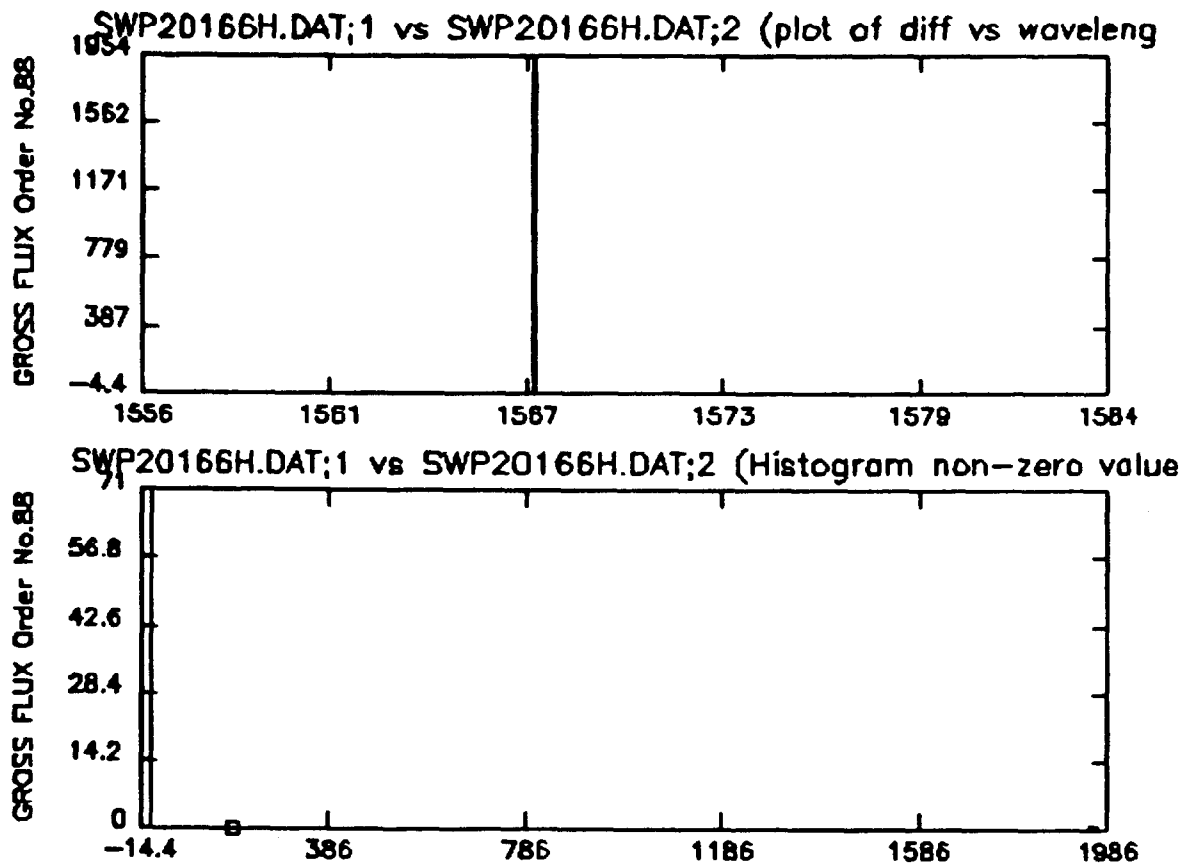


Figure 13: The top plot is the difference in FN in the gross high dispersion spectrum of SWP 20166, order 88, between data processed on the VAX and data processed on the Sigma-9. The y-axis is in units of FN and the x-axis in units of Angstroms. The bottom plot is the histogram of the difference in FN in the gross high dispersion spectrum of SWP 20166, order 88, between data processed on the VAX and data processed on the Sigma-9. The y-axis is number of points and the x-axis is in units of FN difference. A spike of 1954 FN difference is present at 1567 Å, due to precision differences between the two computers.

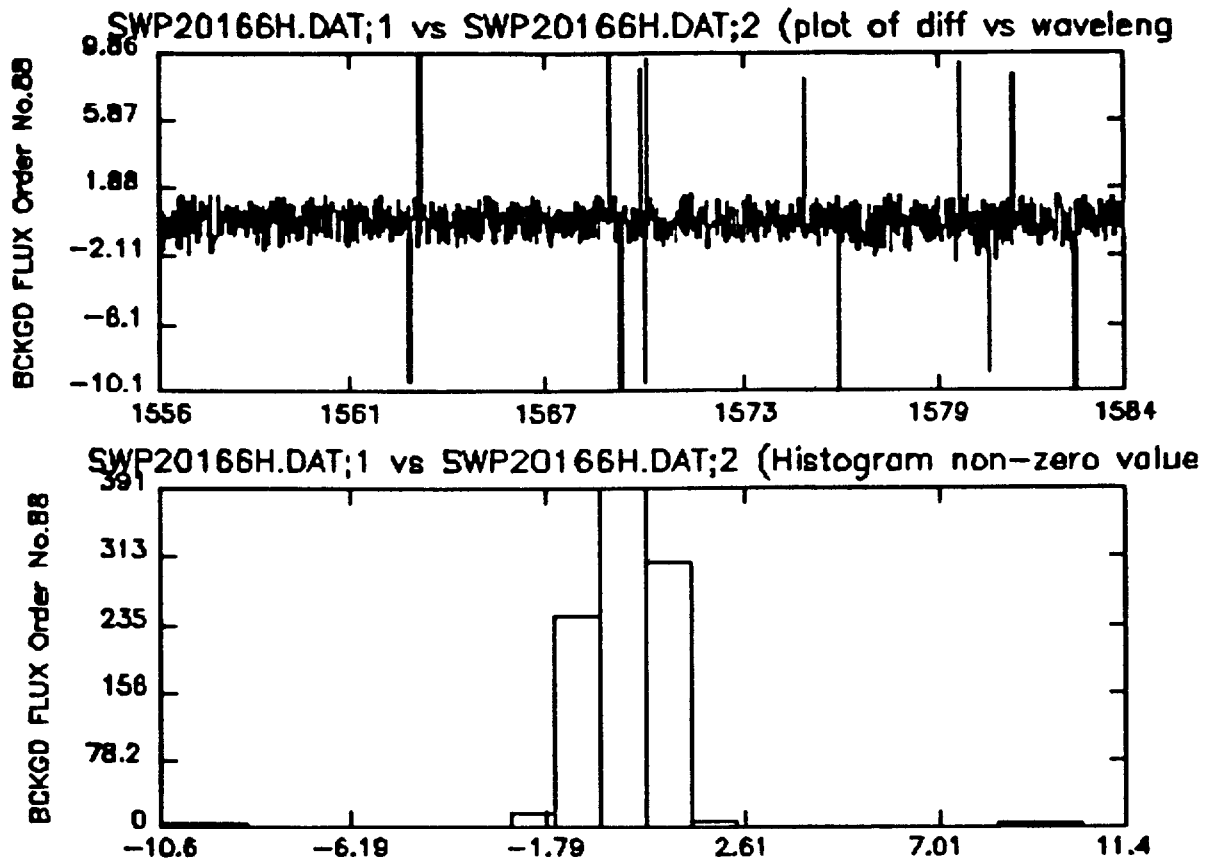


Figure 14: The top plot is the **difference** in FN in the background high dispersion spectrum of SWP 20166, order 88, between data processed on the VAX and data processed on the Sigma-9. The y-axis is in units of FN and the x-axis in units of Angstroms. The bottom plot is the histogram of the **difference** in FN in the background high dispersion spectrum of SWP 20166, order 88, between data processed on the VAX and data processed on the Sigma-9. The y-axis is number of points and the x-axis is in units of FN difference.

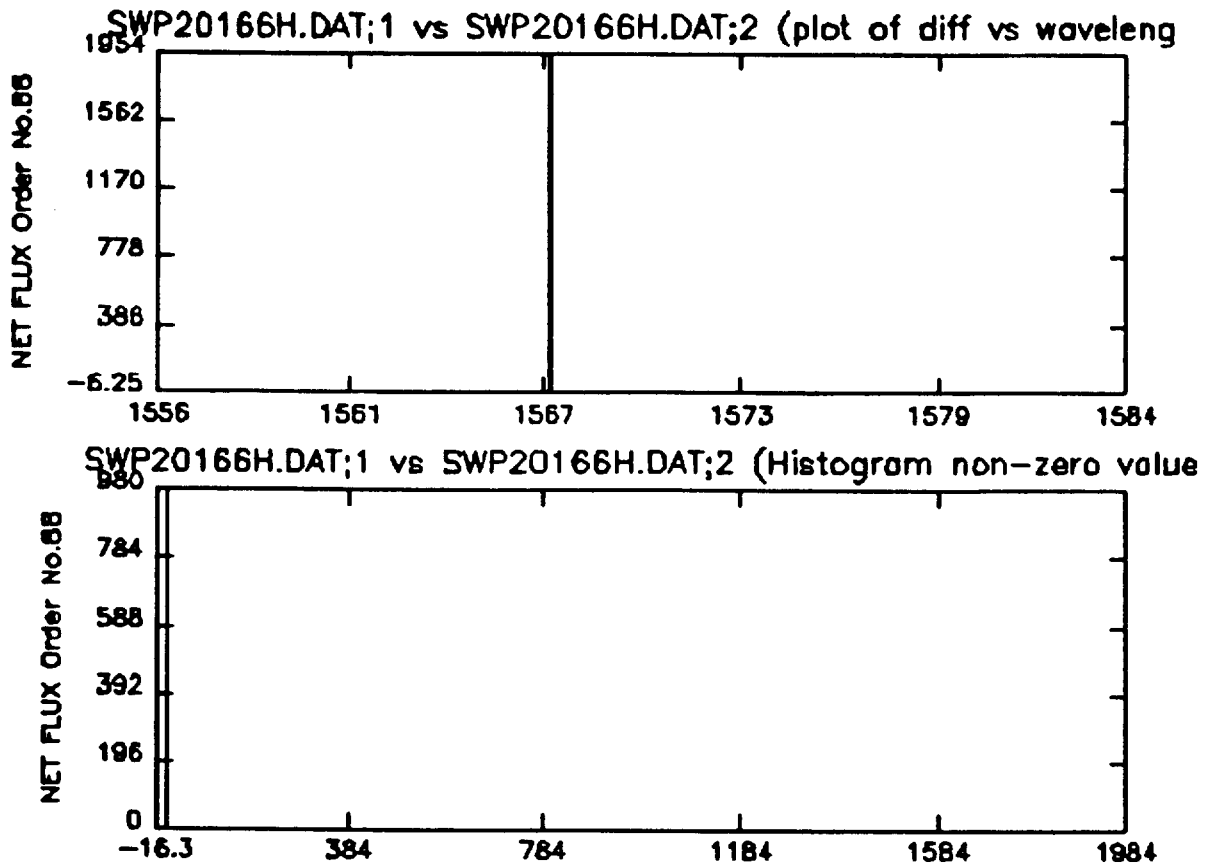


Figure 15: The top plot is the **difference** in FN in the net high dispersion spectrum of SWP 20166, order 88, between data processed on the VAX and data processed on the Sigma-9. The y-axis is in units of FN and the x-axis in units of Angstroms. The bottom plot is the histogram of the **difference** in FN in the background high dispersion spectrum of SWP 20166, order 88, between data processed on the VAX and data processed on the Sigma-9. The y-axis is number of points and the x-axis is in units of FN difference.

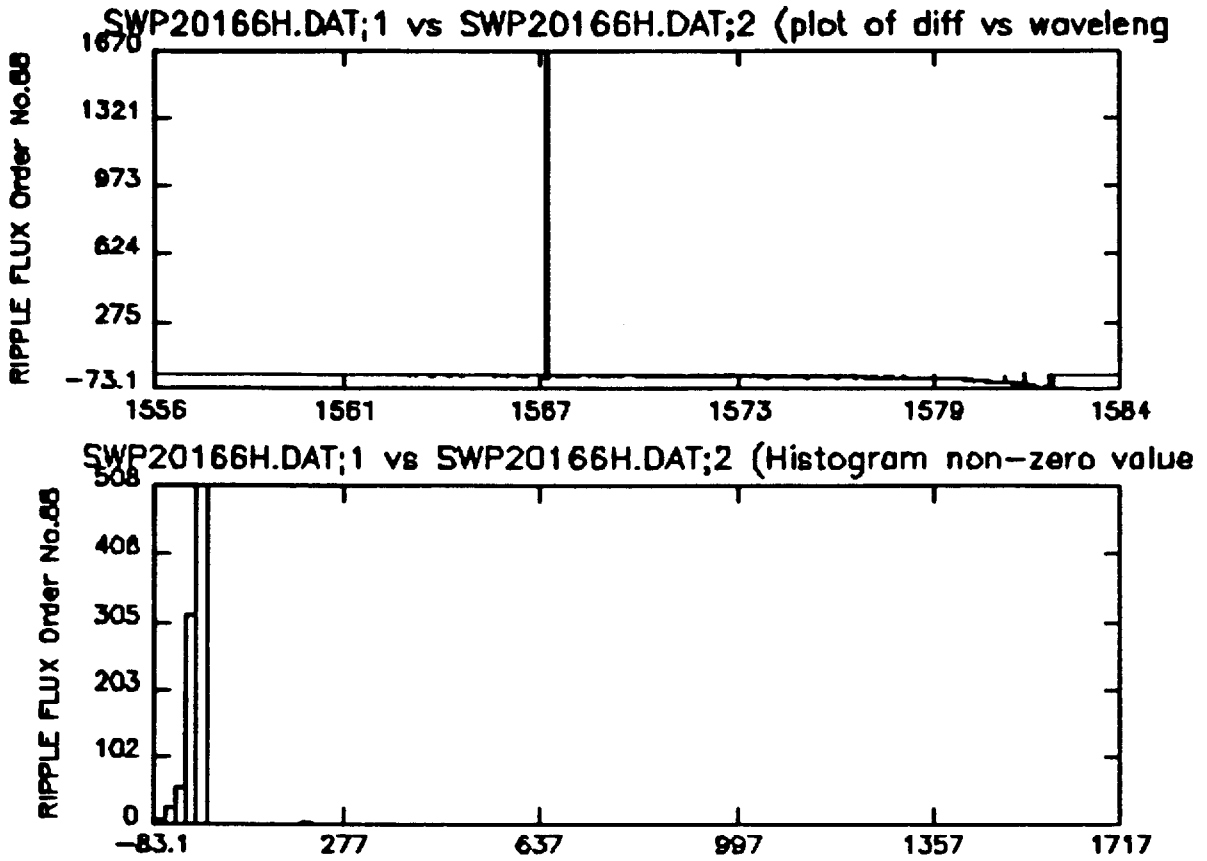


Figure 16: The top plot is the **difference** in FN in the ripple-corrected high dispersion spectrum of SWP 20166, order 88, between data processed on the VAX and data processed on the Sigma-9. The y-axis is in units of FN and the x-axis in units of Angstroms. The bottom plot is the histogram of the **difference** in FN in the ripple-corrected high dispersion spectrum of SWP 20166, order 88, between data processed on the VAX and data processed on the Sigma-9. The y-axis is number of points and the x-axis is in units of FN difference.

Sigma-9 Version

```

POF C** DATA REC. 11 1 1 1 768 8448 5 3 6.1 5.0 2536 .00000 1PC
      0 1684 3374 6873 9091 10586 1PC
      14371 17745 21524 25105 28500 1PC
      11.000 11.000 11.000 11.000 11.000 11.000 1PC
      11.000 11.000 11.000 11.000 11.000 1PC
TUBE 3 SEC EHT 6.1 ITT EHT 5.0 WAVELENGTH 2536 DIFFUSER 0 1PC
      C MODE : FACTOR .178E 00 1PC
*PHOTOM 06:58Z DEC 27,'87 HC
***** DATA FROM LARGE APERTURE ***** C
*ESPECL 06:58Z DEC 27,'87 C
OBSERVATION DATE(GMT): YR=84 DAY= 60 HR=22 MIN=14, (JD): 2445760.4264 C
TARGET COORD (1950) : RT. ASC.= 8 4 43.2 DECL.= 75 6 48 C
OPTIONS :HT=15, HBACK= 5, DISTANCE= 11.0, OMEGA= 90.0 C
MEAN RESEAU (GMT= 84.007-84.204 NO. FF= 94 SIGS= .158 SIGL= .166 PX) C
MEAN DC (GMT= 78.274-84.071 NO. WLC= 107 SIGS= .254 SIGL= .231 PX) C
B 1= -.281791069126D 03 B 2= .376216681767D 00 B 3= .000000000000D 00C
A 1= .967943900643D 03 A 2= -.466574767462D 00 A 3= .000000000000D 00C
THDA FOR RESEAU MOTION = 10.51 C
DN FOR RESEAU MOTION = 50 ( 75, 86, 71, 82) C
THDA FOR SPECTRUM MOTION = 10.84 C
THERMAL SHIFTS: LINE = .649 SAMPLE = 1.551 C
REGISTRATION SHIFTS: LINE = .584 SAMPLE = .471 AUTO C
*POSTLO 06:58Z DEC 27,'87 HC
*****MERGED SPECTRA- GROSS, BACKGROUND, NET, & ABS. CALIB. NET C
*ARCHIVE 07:26Z DEC 27,'87 HL

```

Figure 17: Image processing portion of the header label from an image processed on the Sigma-9 computer.

VAX Version

```

PCF C/** DATA REC. 11 1 1 1 768 8448 5 3 6.1 5.0 2536 .00000 1PC
      0 1684 3374 6873 9091 10586 1PC
      14371 17745 21524 25185 28500 1PC
      11.000 11.000 11.000 11.000 11.000 11.000 1PC
      11.000 11.000 11.000 11.000 11.000 1PC
TUBE 3 SEC EHT 6.1 ITT EHT 5.0 WAVELENGTH 2536 DIFFUSER 0 1PC
C MODE : FACTOR 0.178E+00 1PC
*PHOPERPHOCOR 19:13Z FEB 13, '88 HC
**SCHEME NAME: T3LYAC ** C
*ESL_PERFLNEXT 19:13Z FEB 13, '88 HC
OBSERVATION DATE(GMT): YR=84 DAY= 60 HR=22 MIN=14, (JD): 2445760.4264 C
TARGET COORD (1950) : RT. ASC.= 8 4 43.2 DECL.= 75 6 48 C
OPTIONS :HT=15, HBACK= 5, DISTANCE= 11.0, OMEGA= 90.0 C
MEAN RESEAU (GMT= 84.007-84.204 NO. FF= 94 SIGS= .158 SIGL= .166 PX) C
MEAN DC (GMT= 78.274-84.071 NO. WLC= 107 SIGS= .254 SIGL= .231 PX) C
B 1=-0.281791148274D+03 B 2= 0.376216681767D+00 B 3= 0.000000000000D+00C
A 1= 0.967943834881D+03 A 2=-0.466574767462D+00 A 3= 0.000000000000D+00C
THDA FOR RESEAU MOTION = 10.51 C
DN FOR RESEAU MOTION = 50 ( 75, 86, 71, 82) C
THDA FOR SPECTRUM MOTION = 10.84 C
THERMAL SHIFTS: LINE = 0.649 SAMPLE = 1.551 C
REGISTRATION SHIFTS: LINE = 0.584 SAMPLE = 0.470 AUTO C
*ESL_MERGESPECT 19:13Z FEB 13, '88 HC
**MERGED SPECTRA- GROSS, BACKGROUND, NET, & ABS. CALIB. NET C
**DATA FROM LARGE APERTURE ** C
*GOT_FMTOUTTAPE/GOT_TABCON 20:06Z FEB 13, '88 HL

```

Figure 18: Image processing portion of the header label from an image processed on the VAX computer.